Prostate-Restricted Replicative Adenovirus Expressing Human Endostatin-Angiostatin Fusion Gene Exhibiting Dramatic Antitumor Efficacy

Xiong Li,[1,2,4] You-Hong Liu,[1,4] Sang-Jin Lee,[1,4] Thomas A. Gardner,[1,2,4] Meei-Huey Jeng,[1,3,4] and Chinghai Kao[1,2,4]

Abstract

Purpose: Our previous studies coadministering a replication-deficient adenovirus expressing endostatin and angiostatin fusion gene (EndoAngio) and a prostate-restricted, replication-competent adenovirus (PRRA) showed dramatic antitumor efficacy. This study integrated EndoAngio with an improved PRRA vector to make a single antiangiogenic PRRA, thereby exerting a similarly dramatic antitumor effect with feasibility for future clinical trials.

Experimental Design: We developed an antiangiogenic PRRA with structural improvements. The antitumor efficacy of EndoAngio-PRRA was evaluated in prostate-specific antigen/prostate-specific membrane antigen (PSA/PSMA)-positive, androgen-independent CWR22rv tumor models. The tumor vasculature and cell morphology were observed by dual-photon microscopy. The antiangiogenic effect of EndoAngio delivered by PRRA and the killing activity of EndoAngio-PRRA were evaluated *in vitro*. Virus-inactivated conditioned media from virus-infected PSA/PSMA-positive cells were tested for apoptosis induction in prostate cancer cells.

Results: Our novel EndoAngio-PRRA is a strong antiangiogenic and antitumor agent. Nine of 10 CWR22rv tumors treated by EndoAngio-PRRA completely regressed, with 1 tumor remaining in a dormant status for 26 weeks after treatment. Dual-photon microscopy revealed that EndoAngio-PRRA not only inhibited the development of tumor vasculature but also induced apoptosis in tumor cells. Subsequent *in vitro* study indicated that EndoAngio-PRRA exhibited stronger tumor-specific killing activity than enhanced green fluorescent protein-PRRA, which expresses enhanced green fluorescent protein instead of EndoAngio. Virus-inactivated conditioned medium from EndoAngio-PRRA–infected PSA/PSMA-positive cells induced apoptosis in C4-2 and CWR22rv cells.

Conclusions: EndoAngio-PRRA uniquely combines three distinct antitumor effects to eliminate androgen-independent prostate cancer: antiangiogenesis, viral oncolysis, and apoptosis. This novel antiangiogenic PRRA represents a powerful agent feasible for future clinical trials for prostate cancer therapy.

Prostate cancer is now the leading cancer diagnosis in men, accounting for ~33% of all new cancer diagnoses and an estimated 234,460 new cases in the United States in 2006. The probable reason for the increase is screening compliance and early detection. Roughly 27,350 men will die of this disease in 2006, which is down 10% from 2005, probably attributable in part to higher long-term success treating locally confined prostate cancer (1). However, many patients still present with metastasis at initial diagnosis and many others will go on to experience metastasis. No cure is available for prostate cancer when it becomes hormone refractory (androgen independent) and metastasizes, at which point the disease becomes lethal.

Antiangiogenesis is a promising therapy for prostate cancer, and several antiangiogenic agents are currently under investigation in clinical trials (2–5). In contrast to other conventional therapies that destroy tumor cells directly, antiangiogenic therapy is directed specifically against microvascular endothelial cells that have been recruited into the tumor bed (6). Thus, antiangiogenic therapy does not induce acquired drug resistance (7). Endostatin and angiostatin are the two most potent angiogenesis inhibitors and have shown strong antitumor effects individually (8, 9) and in combination (10–12). However, effective antiangiogenic therapy requires the continuous presence of the inhibitors in the blood and thus needs cycled administration, which is a tremendous challenge technically and economically.

Authors' Affiliations: Departments of [1]Urology, [2]Microbiology and Immunology, and [3]Medicine and [4]Walther Oncology Center, Indiana University School of Medicine, Indianapolis, Indiana

Received 4/11/07; revised 9/19/07; accepted 10/11/07.

Grant support: NIH grants CA074042 and CA118218 (C. Kao); Department of Defense grant W23RX-3270-N729 (C. Kao); and NIH, National Research Service Award Number 1 T32 HL007910, Basic Science Studies on Gene Therapy of Blood Disease (X. Li).

The costs of publication of this article were defrayed in part by the payment of page charges. This article must therefore be hereby marked *advertisement* in accordance with 18 U.S.C. Section 1734 solely to indicate this fact.

Requests for reprints: Chinghai Kao, Department of Urology, Indiana University School of Medicine, 1001 West 10th Street, Room OPW #320, Indianapolis, IN 46202. Phone: 317-278-6873; Fax: 317-278-3432; E-mail: chkao@iupui.edu.

doi:10.1158/1078-0432.CCR-07-0867

Therefore, antiangiogenic therapy is frequently used together with other antitumor agents, such as Taxol (13), to achieve better cancer therapeutic efficacy. In our past studies, we developed a prostate-restricted replicative adenovirus (PRRA; ref. 14) and investigated the synergistic antitumor effect of PRRA combined with a replication-defective adenovirus encoding an endostatin and angiostatin fusion gene (EndoAngio) in androgen-independent prostate cancer (12). We observed that PRRA augmented the transduction effect and expression of antiangiogenic factor, showing a significant antiangiogenic and antitumor effect. The result indicated that combinational therapy using PRRA and antiangiogenesis either eliminated tumors or generated an unhealthy local microenvironment unfavorable for tumor growth. In this report, we developed a novel EndoAngio-PRRA by integrating an EndoAngio expression cassette in PRRA. We observed that EndoAngio-PRRA not only inhibited the development of tumor vasculature but also induced apoptosis in tumor cells, possibly resulting from a unique tumor killing effect of EndoAngio protein delivered by a PRRA.

Materials and Methods

Cells and cell culture. HER911E4, a HER911 (human embryonic retinoblast) derivative with adenoviral *E4* gene under the control of *tetR* (a gift from Leiden University and Crucell, Leiden, the Netherlands; ref. 15), was maintained in DMEM supplemented with 10% fetal bovine serum, 1% penicillin/streptomycin, 0.1 mg/mL hygromycin B (Calbiochem), and 2 μg/mL doxycycline (Sigma). Human umbilical vein endothelial cells (HUVEC) were obtained from Cambrex Bio Science and maintained in endothelial-specific medium EGM-2 (Cambrex Bio Science) according to the manufacturer's instructions. Prostate-specific antigen/prostate-specific membrane antigen (PSA/PSMA)-positive prostate cancer cell lines C4-2 and CWR22rv and negative cells PC-3 and DU145 were all maintained in RPMI 1640 supplemented with 10% fetal bovine serum and 1% penicillin/streptomycin.

Construction of recombinant adenoviruses. The construction system used for EndoAngio-PRRA was developed by Dr. Xavier Danthinne (O.D. 260, Inc., Boise, ID) with some subsequent improvements. Briefly, the present system contains three parts: a cloning vector pAd1020 *Sfi* dA containing adenovirus left inverted terminal repeat and packaging signal (1-358 bp), a modified adenovirus 5 (Ad5) genome backbone vector called E1bF5/35E4 (Δorf 1-4), which contains the Ad5 genome from the E1b TATA box to the E4 TATA box with some modifications, and another cloning vector, called p304 *Sfi*, containing the right-sided inverted terminal repeat (from 35,819 to 35,935 bp) of the adenoviral genome, which allows us to clone the desired genes into the right end of the adenoviral genome. The expression cassette, including hEF1α-HTLV promoter (with activity similar to the cytomegalovirus promoter), human endostatin-angiostatin (EndoAngio) fusion gene, and polyadenylate signal, was excised from pBlast-hEndoAngio expression vector (Invivogen) and subcloned into pAd1020 *Sfi* dA and then cut out from the cloning vector with a kanamycin-resistant gene and a λ phage packaging signal (COS) using restriction enzyme *Sfi*I. On the other side, prostate-specific enhancer sequence (PSES) and *E1a* genes were cloned into p304 *Sfi* to form p304 *Sfi* PSESE1a. Additionally, the Ad5 backbone was modified to release enough space for all the recombinant structures used in the construction. We replaced the Ad5 fiber shaft with an Ad5/35 hybrid fiber shaft, to free up 756 bp, and deleted E4 open reading frames 1 to 4 to release ~1,238 bp. To create our fiber-modified Ad5/35 hybrid vector, we did PCR on a *Nde*I/*Afl*II fragment (1,261 bp) containing Ad5/35 fiber from Ad5EGFP/F35 (a gift from Dr. Andre Lieber, University of Washington, Seattle, WA; ref. 16) and then cloned the fragment into the E1bE4 vector to make E1bF5/35E4. We deleted E4 open reading frames 1 to 4 in E1bF5/35E4 as described by Dr. Hearing to make E1bF5/35E4 (Δorf 1-4) vector (17). These adenoviral vectors were digested by the restriction enzyme *Sfi*I and ligated together. The ligation mixture was used to transform bacteria. After transformation, the bacteria were double selected with ampicillin and kanamycin. Cosmids were isolated from clones containing the right construct. Recombinant adenoviral genomes were released by *Pac*I digestion and transfected into 911E4 cells in the absence of doxycycline. One replication-deficient control virus, RDA, was constructed by deleting the E1a TATA box and another control virus, enhanced green fluorescent protein (EGFP)-PRRA, was constructed by replacing the hEF1α-HTLV promoter-controlled EndoAngio fusion gene expression cassette with cytomegalovirus promoter-controlled EGFP. All cesium chloride–purified adenoviruses were titered by O.D. 260 and plaque formation assay according to the standard protocols.

Flow cytometric analysis (fluorescence-activated cell sorting) to test viral infectivity. CWR22rv, C4-2, PC-3, and DU145 cells were seeded in 12-well plates (2.5×10^5 per well) and infected with replication-deficient adenoviruses Ad5EGFP and Ad5EGFP/F35 or left uninfected 1 day after cell seeding. Each cell line was infected with differing amounts of virus for a similar infectivity (14). Cells were harvested using 0.25% trypsin 24 h after infection, washed with fluorescence-activated cell sorting buffer (PBS with 5% fetal bovine serum and 0.1% sodium azide) on ice, and then fixed in 0.5 mL of cold 1% paraformaldehyde solution for fluorescence-activated cell sorting analysis.

Preparation of conditioned medium and Western blotting. CWR22rv and DU145 cells (4×10^6) were plated in 100-mm culture dishes 24 h before virus infection. The cells were infected by standardized doses of EndoAngio-PRRA. The media were changed 8 h after viral infection. The conditioned medium (CM) was harvested 1 or 3 days after viral infection and concentrated by Centricon YM30 (Millipore). The collected CM were used for testing EndoAngio expression by Western blotting, and the CM collected at 3 days were used for evaluating antiangiogenic activity on HUVEC *in vitro* by cell proliferation, tubular network formation, and cell migration assays. Western blotting was done as described in ref. 12.

Assays of HUVEC cell proliferation, tubular network formation, and cell migration. The experimental methods have been described in detail in ref. 12.

Animal experiments. The CWR22rv tumor model was established by injecting 2×10^6 cells s.c. in flanks of athymic nude mice (6-week-old males). Mice were castrated 3 days after cell injection. Mice were randomly grouped when tumor size reached ~5 mm in diameter at around 2 to 3 weeks after cell injection. The tumors received intratumoral injections of 7×10^8 plaque-forming units of RDA, EGFP-PRRA, or EndoAngio-PRRA in 100 μL 1× PBS by 27-gauge syringe with a needle. Tumor appearance and sizes were monitored once every week and the tumor volumes were calculated by using the following formula: length × width^2 × 0.5236 (18). Mice were sacrificed when tumor size exceeded 1,000 mm^3. One-way ANOVA was used to compare the tumor growth ratios between the treatment groups.

Real-time intravital dual-photon imaging of prostate tumor. Two mice in each group above were injected i.v. with a 100 μL (5 mg/mL) solution of rhodamine-conjugated bovine serum albumin (Molecular Probes) to label blood vessels 4 h before imaging (11) and a 100 μL (0.5 mg/mL) solution of Hoechst 33342 (Molecular probes, Inc.) to label tumor cell nuclei over 2 min to allow identification of all cells and examination of nuclear morphology. The mice were anesthetized and the tumors were exposed by a skin-flap window and covered by a glass-bottom microwell dish (MatTek) bathed in isotonic saline (19). The *in vivo* real-time intravital imaging of tumors was conducted under a Bio-Rad MRC1024 MP laser scanning confocal/multiphoton scanner attached to a Nikon 60× numerical aperture 1.2 water immersion objective lens. Fluorescence excitation was provided by a tunable titanium-sapphire laser (using a 5 W Millennia diode solid state pump

laser). The mice were placed on a heating pad maintained at 37°C in all procedures until recovery. The images were collected as single focal planes, time series or Z-series for volume rending. The images were subsequently analyzed and processed by the MetaMorph program (Universal Imaging Corp.). This approach allows a qualitative assessment of intratumoral vasculature, including the diameter of blood vessels, leaking of tumor vasculature, and differences in the rate of blood flow. The diameters of blood vessels were measured in 20 fields for statistical analysis in each group. In addition, the tumor cell nuclei were observed to detect apoptosis.

Histology, immunohistochemistry, and* in situ *terminal deoxynucleotidyl transferase–mediated dUTP nick end labeling assay. At 21 days after virus injection, tumor samples for real-time intravital dual-photon imaging were harvested, immediately fixed in buffered formalin, processed, embedded in paraffin, and cut into histologic sections. Tumor sections were stained with H&E according to the standard protocol. For blood vessel analysis, a rat monoclonal antibody reactive to mouse CD31 (BD Biosciences PharMingen) and a biotinylated polyclonal anti-rat second antibody (BioGenex) were applied. For the adenovirus infection analysis, mouse monoclonal (SPM 230) antibody (ready for use) to Ad5 E1a (Abcam) and a supersensitive biotinylated second antibody for mouse (BioGenex) were used. The blood vessel morphology was observed by both H&E and CD31 staining. Apoptosis in tumor cells was detected by the DeadEnd fluorometric terminal deoxynucleotidyl transferase–mediated dUTP nick end labeling system (Promega) according to the manufacturer's instructions. The slides were observed under the Bio-Rad MRC1024 MP laser scanning confocal/multiphoton scanner.

Crystal violet cell killing assay. CWR22rv and DU145 cells were seeded in 24-well plates (1×10^5 per well) 1 day before infection. Cells were infected at serial doses ranging from 2.1875 to 35 multiplicities of infection of RDA, EGFP-PRRA, or EndoAngio-PRRA. A row of six-wells

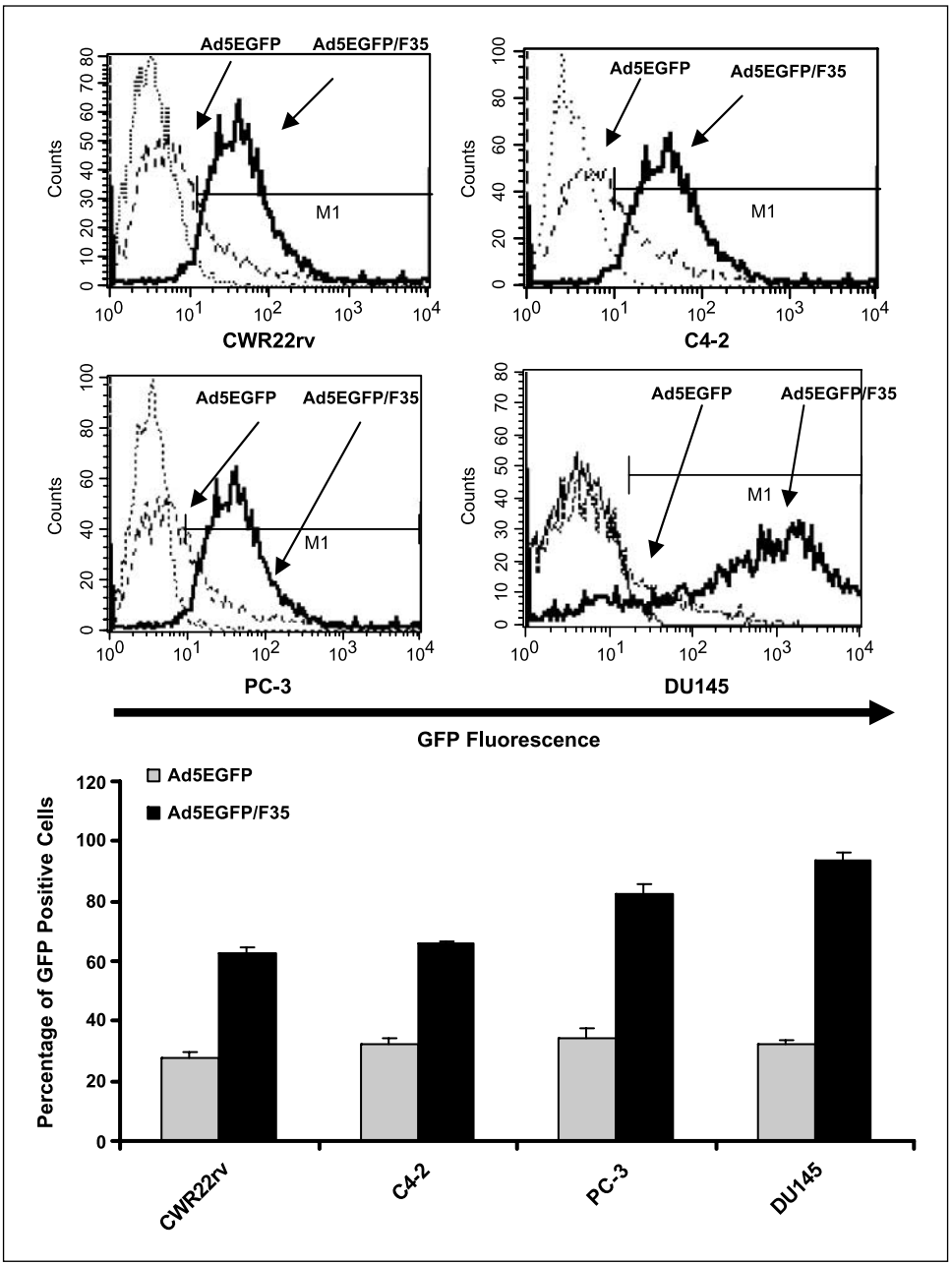

Fig. 1. Ad5 with the Ad5/35 hybrid fiber exhibited higher viral infection ability than that with the Ad5 fiber in prostate cancer cells. CWR22rv, C4-2, PC-3, and DU145 cells were infected with Ad5EGFP and Ad5EGFP/F35 (both are E1/E3-deleted, replication-deficient adenoviruses). The viral doses were adjusted for similar infectivity of Ad5EGFP in individual cell lines. The percentage of virus-infected green fluorescent cells was determined by flow cytometry analysis 24 h after virus infection.

was used for each virus. The growth media were changed every other day. Cells were monitored under the microscope daily and violet crystal assay was then done to detect living cells on day 7 after virus infection (20).

Flow cytometry analysis to detect apoptosis induction by CM-EndoAngio. The viruses in the CM collected from EndoAngio-PRRA–infected and EGFP-PRRA–infected CWR22rv cells were inactivated by heating at 56°C for 30 min (21). Inactivation of virus was confirmed by the disappearance of virus-infected green fluorescent cells when the cells were cocultured with CM-EGFP. Then, C4-2 and CWR22rv cells (1×10^5 per well) were seeded in 24-well plates and cultured with 300 μg protein from the CM, with PBS treatment as a control. Cells were harvested with 0.25% trypsin 72 h after coculture, washed with PBS once, and resuspended in 100 μL PBS. An Annexin V/propidium iodide apoptosis detection kit (BD Biotechnology) was used to detect apoptosis by fluorescence-activated cell sorting analysis.

Results

Adenovirus infectivity is enhanced by the modification of Ad5 fiber to a shorter-sized Ad5/35 hybrid fiber. Our initial reason for fiber modification in the project was that the EndoAngio fusion gene expression cassette is too huge (~2.4 kb) to be packaged in our previous AdE4PSESE1a system successfully (14). In addition to other feasible modification strategies, a 756-bp shorter-sized Ad5/35 hybrid fiber is also an attractive strategy to release enough space for EndoAngio (16, 22). We compared the viral infectivity of Ad5 vector with Ad5/35 hybrid fiber and conventional Ad5 vector in several prostate cancer cell lines. We found that Ad5 vector with Ad5/35 hybrid fiber exhibited higher viral infectivity than Ad5 in all tested prostate cancer cell lines (Fig. 1).

EndoAngio-PRRA is a strong antiangiogenic agent. We generated a novel antiangiogenic PRRA, called EndoAngio-PRRA, by placing an expression cassette of EndoAngio-hEF1α-HTLV on the left arm of the virus and adenoviral *E1a* and *E4* genes, controlled by a novel PSES (23), on the right arm of the virus. The Ad5 fiber was replaced by a shorter-sized Ad5/35 hybrid fiber, and E4 open reading frames 1 to 4 were deleted to release enough space for EndoAngio due to limited Ad5 packaging ability. An EGFP-PRRA–expressing EGFP instead of EndoAngio and an *E1a* TATA box deletion replication-deficient adenovirus RDA were constructed as control viruses (Fig. 2A).

To determine whether the tumor-specific EndoAngio expression delivered by PRRA could be enhanced via virus replication in PSA/PSMA-positive prostate cancer cells but not in the negative cells, we analyzed both cell lysates and CM following the infection of PSA/PSMA-positive CWR22rv and negative DU145 cells with EndoAngio-PRRA. As shown in Fig. 2B,

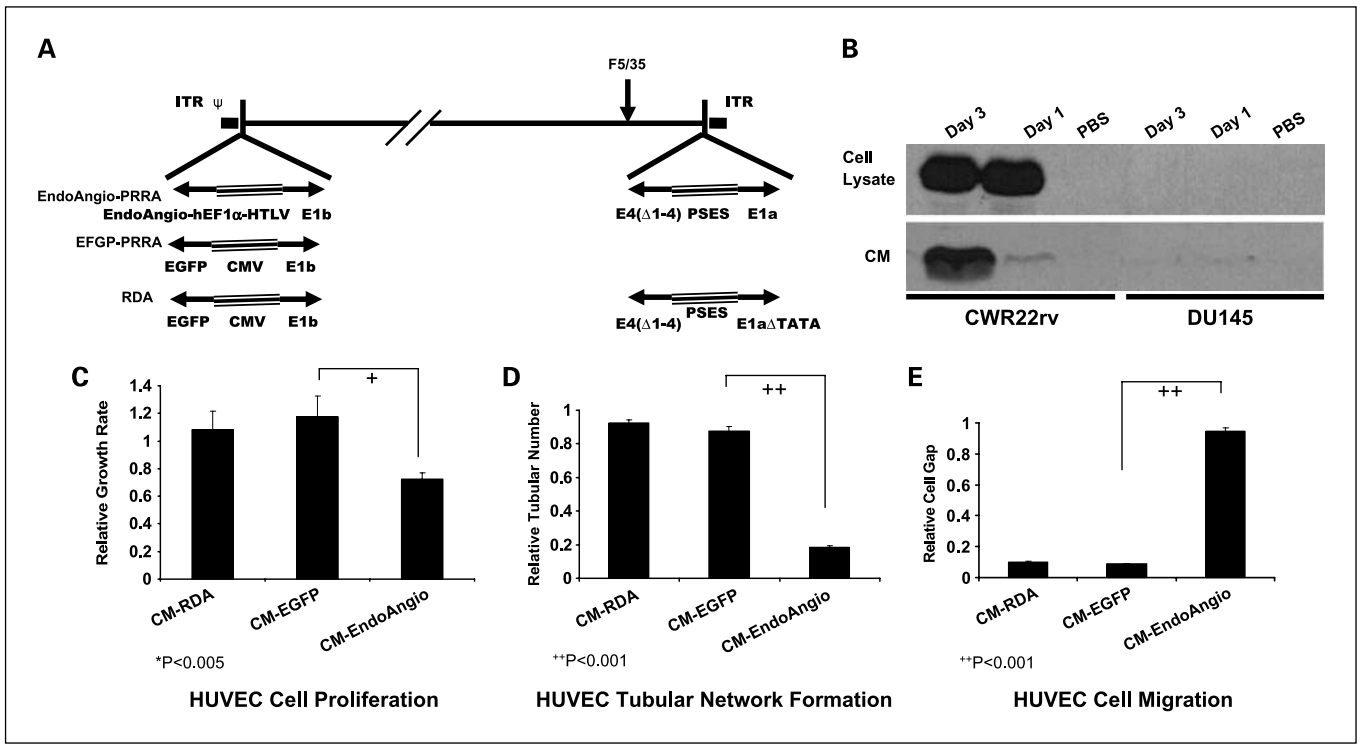

Fig. 2. EndoAngio-PRRA exhibited tumor-specific EndoAngio protein expression and significant antiangiogenesis effect. *A,* scheme of EndoAngio-PRRA. PSES enhancer directs viral replication by controlling the *E1a* and *E4* genes, Ad5 fiber was replaced by Ad5/35 hybrid fiber, and E4 open reading frames 1 to 4 were deleted. An EGFP-PRRA–expressing EGFP instead of EndoAngio and an *E1a* TATA box deletion replication-deficient adenovirus RDA were constructed as control viruses. ITR, inverted terminal repeat; CMV, cytomegalovirus. *B,* CWR22rv and DU145 cells were infected with EndoAngio-PRRA; then, 60 μg protein derived from the cell lysates or CM was subjected to Western blot analysis using an anti-endostatin antibody. The EndoAngio expression in both cell lysates and CM significantly increased with time in the PSA/PSMA-positive CWR22rv, but only faint expression was found in the negative cell DU145, with no increase. *C,* CM harvested from EndoAngio-PRRA–infected CWR22rv (CM-EndoAngio) inhibits HUVEC proliferation. HUVEC cells were treated with CM, and 3-(4,5-dimethylthiazol-2-yl)-2,5-diphenyltetrazolium bromide assay was done after 7 d. Columns, percentage of live cells versus PBS-treated cells of three independent experiments; bars, SD. +, $P < 0.005$. *D,* CM-EndoAngio inhibits HUVEC tubular network formation. The mixtures of HUVEC and CM were dispensed in 24-well plates coated with Matrigel and incubated for 8 h. The tubular network formation was quantified by counting the number of connecting branches between discrete endothelial cells. ++, $P < 0.001$. *E,* CM-EndoAngio inhibits HUVEC migration. A confluent monolayer of HUVEC cells was scratched, displaced cells were removed, and fresh medium containing CM was added. The gap distances were quantified (12), and data are presented as a comparison value (the gap distance at 12 h/initial distance). ++, $P < 0.001$. These results indicated that EndoAngio delivered by PRRA exerted significant antiangiogenic effects *in vitro*.

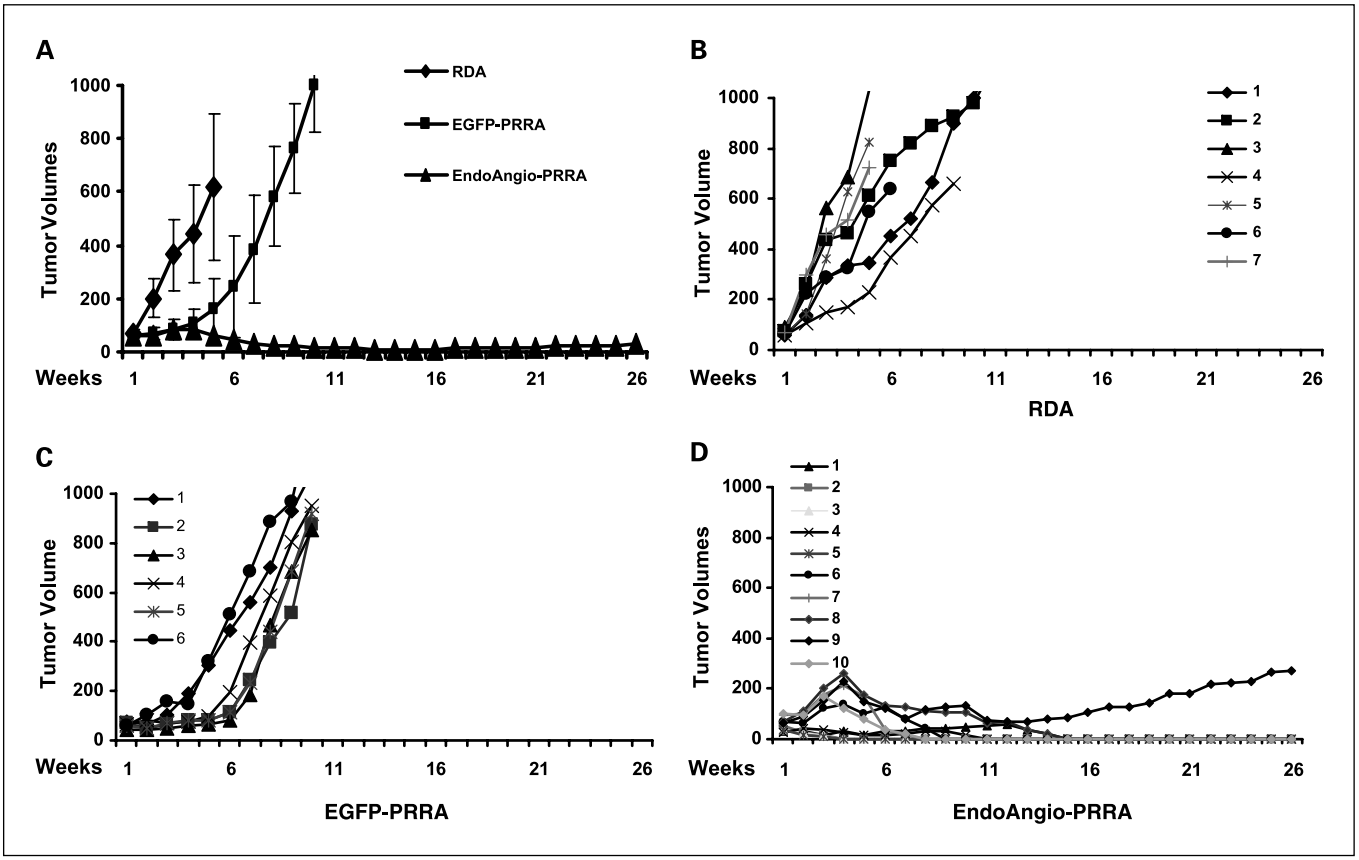

Fig. 3. EndoAngio-PRRA showed significant antitumor effects *in vivo*. CWR22rv s.c. tumors were established in athymic nude mice, and the tumors were treated once by intratumoral injection with 7×10^8 plaque-forming units of RDA, EGFP-PRRA, or EndoAngio-PRRA. Tumor sizes were monitored once every week. Mice were sacrificed when tumor size exceeded 1,000 mm^3. *A,* average tumor sizes of three treatment groups. *B* to *D,* individual tumor sizes of three treatment groups. Nine of 10 tumors treated by EndoAngio-PRRA were eliminated completely at 15 wk and 1 tumor remained dormant for 26 wk after treatment.

EndoAngio protein expression was detected in CWR22rv cells just 1 day after virus infection, and similar expression was seen on day 3, but no detectable protein was found in DU145 on either day 1 or day 3. In the CM harvested from EndoAngio-PRRA–infected CWR22rv, more EndoAngio expression was detected on day 3 than on day 1. Only very faint protein expression could be detected in CM from DU145 on day 1, and no increase was found on day 3. These results showed that EndoAngio-PRRA resulted in a high level of tumor cell type-restricted transgene expression of EndoAngio in PSA/PSMA-positive prostate cancer cells.

Cell proliferation assay [3-(4,5-dimethylthiazol-2-yl)-2,5-diphenyltetrazolium bromide assay], tubular network formation assay (Matrigel assay), and cell migration assay were done to test the antiangiogenic activity of EndoAngio-PRRA using the CM described above. CM from EndoAngio-PRRA–infected CWR22rv (CM-EndoAngio) significantly inhibited HUVEC proliferation compared with CM from the control virus EGFP-PRRA–infected CWR22rv (CM-EGFP; $P < 0.005$; Fig. 2C). Assays of *in vitro* tubular network formation also confirmed that CM-EndoAngio had a stronger inhibitory effect on tubular network formation of HUVEC cells than CM-EGFP or CM-RDA ($P < 0.001$; Fig. 2D). CM-EndoAngio had a stronger inhibitory effect on the migration of HUVEC cells than CM-RDA or CM-EGFP ($P < 0.001$; Fig. 2E). Collectively, these results clearly showed that EndoAngio protein delivered by PRRA exerted a significant antiangiogenic effect on HUVEC proliferation, tubular network formation, and cell migration.

EndoAngio-PRRA exhibited strong antitumor efficacy. We evaluated the antitumor efficacy of EndoAngio-PRRA on the growth of androgen-independent CWR22rv s.c. tumors in athymic mice (Fig. 3A). Compared with the tumor growth in the animal tumors treated by RDA (Fig. 3B), EGFP-PRRA only delayed tumor growth in the first 4 to 6 weeks, after which most of the treated tumors grew exponentially (Fig. 3C). On the other hand, EndoAngio-PRRA resulted in complete regression of 9 of 10 androgen-independent CWR22rv tumors in castrated nude mice at 15 weeks after treatment, and 1 further tumor remained dormant until 26 weeks after virus injection (Fig. 3D).

We observed a dark blue color on the tumor skin of 8 of 10 EndoAngio-PRRA–treated tumors at 15 to 21 days after virus injections, which indicated probable necrosis and hemorrhage inside the tumors. The remaining two tumors still exhibited dark blue 70 days after treatment. The tumors treated by RDA and EGFP-PRRA did not develop blue coloration (Fig. 4A). Five EndoAngio-PRRA–treated tumors exhibited skin ulceration and even bleeding; then, four tumors flattened and were absorbed, whereas one tumor remained at a small size for a long time. In contrast to the vasculature inside the EGFP-PRRA–treated tumors at day 5 after virus injection, real-time intravital dual-photon imaging showed that the blood vessels

labeled by rhodamine-conjugated bovine serum albumin inside the EndoAngio-PRRA–treated tumors had thinner diameters, and some blood vessel sections exhibited stenotic blood passageways with single blood cells distinguished clearly, which indicated that blood flow was nearly stagnant and almost negligible. At 21 days after treatment, the diameter of the blood vessels decreased further with less dye leaking outside the vasculature inside tumors. In contrast, large straight blood vessels were observed in the control tumors on both day 5 and day 21. The vessel diameters were measured and showed a significant difference ($P < 0.001$). The tumors were harvested for H&E staining and CD31 immunohistochemical staining at 21 days to observe the blood vessels inside tumors. The morphology of blood vessels was consistent with the findings by dual-photon microscope (Fig. 4B). Direct evidence from living animal tumors revealed the significant antiangiogenic therapeutic efficacy of EndoAngio-PRRA administration in this androgen-independent prostate cancer animal model.

Tumors treated by EndoAngio-PRRA presented distinct pathologic features. Five of 10 tumor xenografts grew in the first 3 weeks after treatment by EndoAngio-PRRA, and then tumor growth was inhibited until tumor regression (Fig. 3D), which suggested that the tumor inhibition efficacy is not simply an effect of antiangiogenesis, which only inhibits tumor growth temporarily (12). To better understand how EndoAngio-PRRA eliminated tumors *in situ*, we injected Hoechst 33343 dye systemically to label cell nuclei to monitor apoptosis during EndoAngio-PRRA treatment using real-time intravital

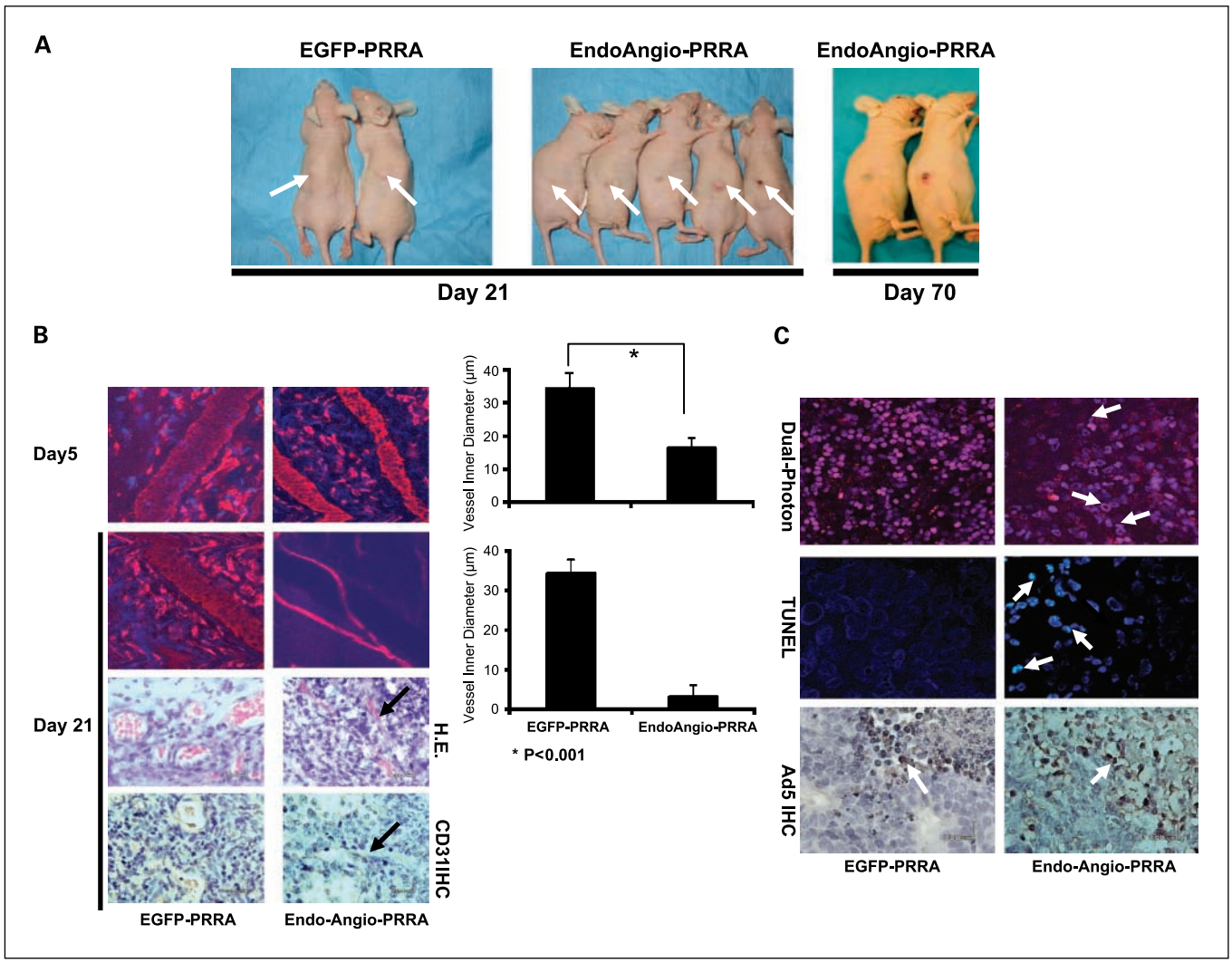

Fig. 4. Administration of EndoAngio-PRRA resulted in inhibition in tumor vasculature and apoptosis in more tumor cells. *A,* CWR22rv s.c tumors treated by EndoAngio-PRRA exhibited dark blue color (*arrows*), which indicated necrosis and hemorrhage inside the tumors. *B,* in EndoAngio-PRRA – treated tumors, some blood vessel sections exhibited thin diameters and stenotic blood passageways with single blood cells distinguished clearly 5 d after treatment. The diameter of blood vessels decreased further with less dye leaking outside the vasculature inside tumors 21 d after treatment ($P < 0.001$). H&E and CD31 immunohistochemical staining of tumor tissues (*arrows*) confirmed the dual-photon microscope findings. *C,* in contrast to EGFP-PRRA, more cell nuclei in EndoAngio-PRRA – treated tumors exhibited nuclear shrinkage and fragmentation and other cells exhibited nuclear enlargement and irregularity (*arrows*), which suggested that the cells were unhealthy or dying. Arrows, terminal deoxynucleotidyl transferase – mediated dUTP nick end labeling – positive staining apoptotic cells in EndoAngio-PRRA – treated tumors were detected. Adenovirus-infected tumor cells, positively labeled by anti-Ad5 E1a antibody (*arrows*), were very similar inside EndoAngio-PRRA – treated and EGFP-PRRA – treated tumors, which suggested similar virus infectivity and distribution with both viruses, but the apoptosis induction of EndoAngio-PRRA is superior to EGFP-PRRA. TUNEL, terminal deoxynucleotidyl transferase – mediated dUTP nick end labeling; IHC, immunohistochemistry.

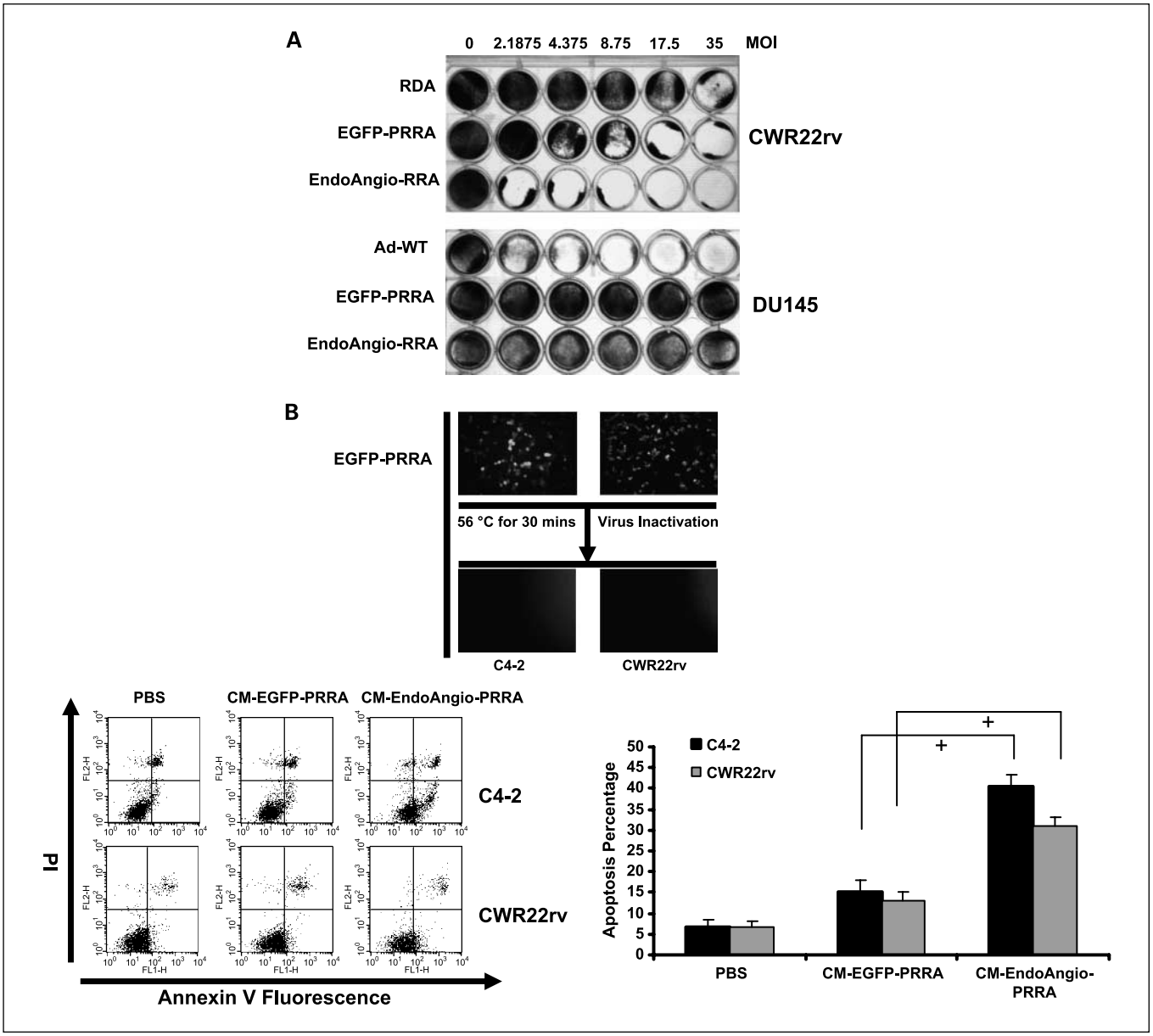

Fig. 5. EndoAngio-PRRA exerted higher tumor-specific killing activity for PSA/PSMA-positive CWR22rv but not for negative DU145. *A,* CWR22rv and DU145 cells were infected with EndoAngio-PRRA and control viruses at stepwise virus doses. WT, wild-type; MOI, multiplicity of infection. A crystal violet assay was done to evaluate virus killing activity at day 7 after virus infection. *B,* the viruses were inactivated, and virus inactivation was confirmed by the disappearance of virus-infected green fluorescent cells when the cells were treated with CM-EGFP. Then, C4-2 and CWR22rv cells were cultured with 300 μg protein from the CM. The apoptotic cells were determined by Annexin V/propidium iodide (*PI*) staining followed by flow cytometry analysis 72 h after coculture. The data suggested that EndoAngio, or EndoAngio-PRRA – infected PSA/PSMA-positive cells, secreted factor(s) that induced apoptosis in prostate cancer cells.

dual-photon microscopy 21 days after treatment. The majority of cell nuclei (blue colors in Fig. 4C) in the EGFP-PRRA–treated tumors were round-oval shaped, indicating a "healthy" tumor condition. The tumor cells in the RDA-treated group showed no significant abnormal morphology (data not shown). In contrast to EGFP-PRRA, cell nuclei in the EndoAngio-PRRA–treated tumors exhibited nuclear shrinkage and even nuclear fragmentation. Other cells exhibited nuclear enlargement and irregularity (Fig. 4C), which suggested that the cells were unhealthy or dying.

We confirmed the dual-photon microscope findings by conducting a DeadEnd fluorometric assay on paraffin-embedded tumor tissue slides harvested at 21 days. In contrast to the tumors treated by EGFP-PRRA, more green apoptotic cells were found inside EndoAngio-PRRA–treated tumors with nuclear fragmentation, although profuse anti-adenovirus E1a antibody staining in dark brown cells (arrows) was detected at a similar level inside EndoAngio-PRRA–treated and EGFP-PRRA–treated tumors (Fig. 4C), which suggested that EndoAngio-PRRA and EGFP-PRRA have similar virus infection and distribution *in vivo*, although EndoAngio-PRRA induces greater tumor cell apoptosis.

EndoAngio-PRRA exhibited higher tumor-specific killing activity than the control virus. The results of EndoAngio-PRRA

treatment *in vivo* showed the stronger antitumor effect and apoptosis induction ability of EndoAngio-PRRA compared with control viruses. Therefore, we tested the tumor-specific cell killing activity of EndoAngio-PRRA *in vitro*. Figure 5A shows that the killing activity of EndoAngio-PRRA is superior to EGFP-PRRA on PSA/PSMA-positive CWR22rv. The killing activity of EGFP-PRRA is superior to RDA, likely due to the replication-competent efficiency of EGFP-PRRA. Not much cellular killing by EGFP-PRRA and EndoAngio-PRRA was found in the PSA/PSMA-negative DU145, although the same doses of wild-type adenovirus generated significant cell killing. This result shows that the killing activity of EndoAngio-PRRA is superior to that of EGFP-PRRA in PSA/PSMA-positive prostate cancer cells, which suggested that EndoAngio protein itself, or other factors produced by the combination of EndoAngio with PRRA, probably had direct cytotoxicity or induced apoptosis in tumor cells.

CM from EndoAngio-PRRA–infected, PSA/PSMA-positive cells induced apoptosis in prostate cancer cells. We did an apoptosis assay culturing C4-2 and CWR22rv cells with virus-inactivated CM. The viruses in the collected CM were inactivated by heating at 56°C for 30 min (21). Virus inactivation was confirmed by the disappearance of virus-infected green fluorescent cells when the cells were cultured with CM-EGFP. In both cell lines, the cell numbers with both Annexin V-FITC and propidium iodide–positive labeling increased significantly when C4-2 or CWR22rv cells were cultured with CM-EndoAngio. The results suggested that EndoAngio-PRRA–infected PSA/PSMA-positive cells secreted factor(s) that induced apoptosis in prostate cancer cells (Fig. 5B).

Discussion

Endostatin, a COOH-terminal proteolytic fragment of collagen XVIII, blocks endothelial cell proliferation, migration/invasion, and tubular network formation *in vitro* and inhibits tumor growth and angiogenesis in a wide variety of animal tumor models with little toxicity, immunogenicity, and resistance (9, 24). Angiostatin, an NH_2-terminal fragment comprising kringles 1 to 3 of plasminogen, also shows potent antiangiogenic (8) and/or antitumor effects (25, 26). Recently, an endostatin and angiostatin fusion protein, EndoAngio, has been developed that exhibits prolonged half-life and greater antiangiogenic and antitumor effects (13, 27).

Adenovirus-mediated gene therapy has been tested broadly in clinical trials, and tumor/tissue-restricted replicative adenovirus showed significant advantages over replication-deficient adenovirus (14, 28, 29). However, the single administration of PRRA ultimately results in failure due to inefficient viral distribution in tumor masses (12, 14). Recently, we reported that androgen-independent CWR22rv s.c. tumor xenografts regressed after a combination therapy using replication-deficient AdEndoAngio expressing EndoAngio and a PRRA, AdE4PESEE1a (12), which suggested that the combination of a PRRA and EndoAngio protein had dramatic synergistic antitumor effects.

Therefore, we designed EndoAngio-PRRA to deliver an endostatin-angiostatin fusion gene for androgen-independent prostate cancer treatment. EndoAngio-PRRA exhibited excellent antitumor effects; 9 of 10 tumors regressed completely 15 weeks after treatment and 1 tumor remained in a dormant status for 26 weeks. Eight of 10 EndoAngio-PRRA–treated tumors developed venous blood stasis, and ultimately 5 of 10 tumors exhibited skin ulceration and necrosis, after which the tumor was promptly eliminated. At days 5 and 21 after virus injection, real-time intravital dual-photon imaging showed that blood vessels inside the EndoAngio-PRRA–treated tumors had thinner diameters, and blood flow was nearly stagnant and almost negligible in some blood vessel sections. These pathologic features were rarely detected in the control virus-treated tumor masses. The results provided us with direct evidence of the ability of EndoAngio-PRRA to decrease tumor blood supply and inhibit the tumor vasculature.

Five of 10 tumors treated by EndoAngio-PRRA grew in the first 3 weeks after treatment and then regressed completely. We believe that the strong tumor inhibition efficacy may involve another mechanism in addition to viral replication and antiangiogenesis. Our previous studies suggested that the combinational therapy of PRRA and AdEndoAngio generated an unhealthy tumor microenvironment that might be toxic to tumor cells (12). Therefore, we evaluated tumor cell apoptosis inside the tumors. In contrast to the plain PRRA-treated tumors, the numbers of apoptotic tumor cells, revealed by both real-time intravital dual-photon imaging and terminal deoxynucleotidyl transferase–mediated dUTP nick end labeling assay in tumor tissue sections, increased significantly in EndoAngio-PRRA–treated tumors, although virus-infected cells labeled by anti-Ad5 E1a antibodies were found at a similar level. The results indicated that virus infection and distribution of EndoAngio-PRRA are similar to EGFP-PRRA inside tumors, but EndoAngio-PRRA induced more tumor cell apoptosis.

The intriguing question is why EndoAngio-PRRA induced more cell apoptosis than plain EGFP-PRRA. We found that the tumor-specific cell killing activity of EndoAngio-PRRA is better than the control adenovirus EGFP-PRRA for CWR22rv cells *in vitro*. Furthermore, virus-inactivated CM containing EndoAngio protein had a significant apoptosis-inducing effect in C4-2 and CWR22rv prostate cancer cells. The results indicated that EndoAngio protein, in addition to the antiangiogenic effect, also exhibited direct cytotoxic or apoptotic effects on androgen-independent prostate cancer tumor cells, and the combination of oncolytic PRRA and EndoAngio had dramatic tumor killing effects. Chi and Pizzo (30) reported recently that angiostatin is directly cytotoxic to tumor cells at low extracellular pH through cell surface–associated ATP synthase. As we know, the local environment would acidify due to rapid adenovirus propagation. The acidified local environment would enhance the apoptosis induction activity and toxicity of EndoAngio. Additionally, endostatin also could have direct anticancer action, although it seems to be restricted to a colon cancer cell line (21). Therefore, the synergistic antitumor efficacy improved dramatically when EndoAngio protein was combined with a PRRA.

In conclusion, we have developed an EndoAngio-PRRA for androgen-independent prostate cancer that was able to eliminate 9 of 10 treated s.c. tumors. Synergistically, three antitumor effects combine to eliminate the whole tumor mass: endostatin-angiostatin that limited tumor growth by inhibiting the tumor vasculature and inducing venous blood stasis inside the tumors, PRRA that effectively infected and killed tumor cells directly,

and EndoAngio that induced apoptosis in prostate cancer cells via viral replication. The *in vivo* therapeutic efficacy we showed suggests that antiangiogenic PRRA is a promising treatment strategy for androgen-independent prostate cancer, which currently has no cure.

Acknowledgments

We thank Barbara A. Sturonas-Brown (Indiana Center for Biological Microscopy) for the technical support of the multiphoton imaging and Dr. Pierrie Dagher, Dr. Kenneth W. Dunn (Indiana Center for Biological Microscopy), and Dr. Shaobo Zhang (Department of Pathology) for the discussions on the multiphoton image analysis.

References

1. Jemal A, Siegel R, Ward E, et al. Cancer statistics, 2006. CA Cancer J Clin 2006;56:106–30.
2. Jin RJ, Kwak C, Lee SG, et al. The application of an anti-angiogenic gene (thrombospondin-1) in the treatment of human prostate cancer xenografts. Cancer Gene Ther 2000;7:1537–42.
3. Sun J, Blaskovich MA, Jain RK, et al. Blocking angiogenesis and tumorigenesis with GFA-116, a synthetic molecule that inhibits binding of vascular endothelial growth factor to its receptor. Cancer Res 2004;64:3586–92.
4. Sweeney P, Karashima T, Kim SJ, et al. Anti-vascular endothelial growth factor receptor 2 antibody reduces tumorigenicity and metastasis in orthotopic prostate cancer xenografts via induction of endothelial cell apoptosis and reduction of endothelial cell matrix metalloproteinase type 9 production. Clin Cancer Res 2002;8:2714–24.
5. Hurwitz H, Fehrenbacher L, Novotny W, et al. Bevacizumab plus irinotecan, fluorouracil, and leucovorin for metastatic colorectal cancer. N Engl J Med 2004;350:2335–42.
6. Folkman J. Antiangiogenic gene therapy. Proc Natl Acad Sci U S A 1998;95:9064–6.
7. Jimenez JA, Kao C, Raikwar S, Gardner TA. Current status of anti-angiogenesis therapy for prostate cancer. Urol Oncol 2006;24:260–8.
8. O'Reilly MS, Holmgren L, Shing Y, et al. Angiostatin: a novel angiogenesis inhibitor that mediates the suppression of metastases by a Lewis lung carcinoma. Cell 1994;79:315–28.
9. O'Reilly MS, Boehm T, Shing Y, et al. Endostatin: an endogenous inhibitor of angiogenesis and tumor growth. Cell 1997;88:277–85.
10. Scappaticci FA, Contreras A, Smith R, et al. Statin-AE: a novel angiostatin-endostatin fusion protein with enhanced antiangiogenic and antitumor activity. Angiogenesis 2001;4:263–8.
11. Raikwar SP, Temm CJ, Raikwar NS, Kao C, Molitoris BA, Gardner TA. Adenoviral vectors expressing human endostatin-angiostatin and soluble Tie2: enhanced suppression of tumor growth and antiangiogenic effects in a prostate tumor model. Mol Ther 2005;12:1091–100.
12. Li X, Raikwar SP, Liu YH, et al. Combination therapy of androgen-independent prostate cancer using a prostate restricted replicative adenovirus and a replication-defective adenovirus encoding human endostatin-angiostatin fusion gene. Mol Cancer Ther 2006;5:676–84.
13. Isayeva T, Ren C, Ponnazhagan S. Intraperitoneal gene therapy by rAAV provides long-term survival against epithelial ovarian cancer independently of survivin pathway. Gene Ther 2007;14:138–46.
14. Li X, Zhang YP, Kim HS, et al. Gene therapy for prostate cancer by controlling adenovirus E1a and E4 gene expression with PSES enhancer. Cancer Res 2005;65:1941–51.
15. He TC, Zhou S, da Costa LT, Yu J, Kinzler KW, Vogelstein B. A simplified system for generating recombinant adenoviruses. Proc Natl Acad Sci U S A 1998;95:2509–14.
16. Shayakhmetov DM, Papayannopoulou T, Stamatoyannopoulos G, Lieber A. Efficient gene transfer into human CD34(+) cells by a retargeted adenovirus vector. J Virol 2000;74:2567–83.
17. Huang MM, Hearing P. Adenovirus early region 4 encodes two gene products with redundant effects in lytic infection. J Virol 1989;63:2605–15.
18. Gleave M, Hsieh JT, Gao CA, von Eschenbach AC, Chung LW. Acceleration of human prostate cancer growth *in vivo* by factors produced by prostate and bone fibroblasts. Cancer Res 1991;51:3753–61.
19. Kelly KJ, Sandoval RM, Dunn KW, Molitoris BA, Dagher PC. A novel method to determine specificity and sensitivity of the TUNEL reaction in the quantitation of apoptosis. Am J Physiol Cell Physiol 2003;284:C1309–18.
20. Hemminki A, Belousova N, Zinn KR, et al. An adenovirus with enhanced infectivity mediates molecular chemotherapy of ovarian cancer cells and allows imaging of gene expression. Mol Ther 2001;4:223–31.
21. Dkhissi F, Lu H, Soria C, et al. Endostatin exhibits a direct antitumor effect in addition to its antiangiogenic activity in colon cancer cells. Hum Gene Ther 2003;14:997–1008.
22. Seshidhar Reddy P, Ganesh S, Limbach MP, et al. Development of adenovirus serotype 35 as a gene transfer vector. Virology 2003;311:384–93.
23. Lee SJ, Kim HS, Yu R, et al. Novel prostate-specific promoter derived from PSA and PSMA enhancers. Mol Ther 2002;6:415–21.
24. Blezinger P, Wang J, Gondo M, et al. Systemic inhibition of tumor growth and tumor metastases by intramuscular administration of the endostatin gene. Nat Biotechnol 1999;17:343–8.
25. Griscelli F, Li H, Bennaceur-Griscelli A, et al. Angiostatin gene transfer: inhibition of tumor growth *in vivo* by blockage of endothelial cell proliferation associated with a mitosis arrest. Proc Natl Acad Sci U S A 1998;95:6367–72.
26. Griscelli F, Li H, Cheong C, et al. Combined effects of radiotherapy and angiostatin gene therapy in glioma tumor model. Proc Natl Acad Sci U S A 2000;97:6698–703.
27. Sun X, Qiao H, Jiang H, et al. Intramuscular delivery of antiangiogenic genes suppresses secondary metastases after removal of primary tumors. Cancer Gene Ther 2005;12:35–45.
28. Li X, Jung C, Liu YH, et al. Anti-tumor efficacy of a transcriptional replication-competent adenovirus, Ad-OC-E1a, for osteosarcoma pulmonary metastasis. J Gene Med 2006;8:679–89.
29. Li X, Zhang J, Gao H, et al. Transcriptional targeting modalities in breast cancer gene therapy using adenovirus vectors controlled by α-lactalbumin promoter. Mol Cancer Ther 2005;4:1850–9.
30. Chi SL, Pizzo SV. Angiostatin is directly cytotoxic to tumor cells at low extracellular pH: a mechanism dependent on cell surface-associated ATP synthase. Cancer Res 2006;66:875–82.

Clinical Cancer Research

Prostate-Restricted Replicative Adenovirus Expressing Human Endostatin-Angiostatin Fusion Gene Exhibiting Dramatic Antitumor Efficacy

Xiong Li, You-Hong Liu, Sang-Jin Lee, et al.

Clin Cancer Res 2008;14:291-299.